Inorganic Chemistry

Article

pubs.acs.org/IC

Chiral Induction at Octahedral Ru(II) via the Disassembly of Diruthenium(II,III) Tetracarboxylates Using a Variety of Chiral Diphosphine Ligands

Brandon R. Groves,[†] D. Ian Arbuckle,[†] Ernest Essoun,[†] Travis L. Lundrigan,[†] Ruiyao Wang,[‡] and Manuel A. S. Aquino*,[†]

[†]Department of Chemistry, St. Francis Xavier University, P.O. Box 5000, Antigonish, Nova Scotia, B2G 2W5, Canada

[‡]Department of Chemistry, Queen's University, 90 Bader Lane, Kingston, Ontario, K7L 3N6, Canada

Supporting Information

ABSTRACT: Achiral $[Ru_2(\mu\text{-}O_2CR)_4(MeOH)_2](PF_6)$ (R = CH_3 or C_6H_5) reacts with the chiral diphosphines *R,R*- and *S,S*-Chiraphos (two chiral centers on ligand between the coordinating P atoms) and *R*-Prophos (one chiral center on ligand between the coordinating P atoms) leading to a disassembly of the paddlewheel core and the highly diastereoselective production of Λ-$[Ru(\eta^2\text{-}O_2CC_6H_5)(\eta^2\text{-}R,R\text{-Chiraphos})_2](PF_6)$ (**Λ-*R,R*-III**), Δ-$[Ru(\eta^2\text{-}O_2CC_6H_5)(\eta^2\text{-}S,S\text{-Chiraphos})_2](PF_6)$ (**Δ-*S,S*-III**) (the R = CH_3 complexes of Chiraphos were reported in a earlier communication in this journal), and Λ-$[Ru(\eta^2\text{-}O_2CCH_3)(\eta^2\text{-}R\text{-Prophos})_2](PF_6)$ (**Λ-*R,R*-VI**), respectively, in high yield and purity. Reactions of the same starting material with *R,R*- and *S,S*-*o-tolyl*-Dipamp (chiral centers *are* the coordinating P-atoms) lead to an inversion in the chirality-at-metal producing Λ-$[Ru(\eta^2\text{-}O_2CC_6H_5)(\eta^2\text{-}S,S\text{-}o\text{-}tolyl\text{-Dipamp})_2](PF_6)$ (**Λ-*S,S*-IV**), Δ-$[Ru(\eta^2\text{-}O_2CC_6H_5)(\eta^2\text{-}R,R\text{-}o\text{-}tolyl\text{-Dipamp})_2](PF_6)$ (**Δ-*R,R*-IV**), Λ-$[Ru(\eta^2\text{-}O_2CCH_3)(\eta^2\text{-}S,S\text{-}o\text{-}tolyl\text{-Dipamp})_2](PF_6)$ (**Λ-*S,S*-V**), and Δ-$[Ru(\eta^2\text{-}O_2CCH_3)(\eta^2\text{-}R,R\text{-}o\text{-}tolyl\text{-Dipamp})_2](PF_6)$ (**Δ-*R,R*-V**). X-ray crystallography of all but **Λ-*S,S*-V** and **Δ-*R,R*-V** and solid-state circular dichroism (CD) show that only the indicated diastereomers are present in the solid-state. Solution CD measurements and ^{31}P NMR also indicate their predominance in solution.

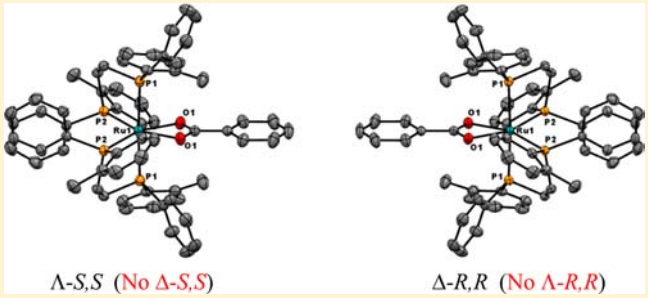

1. INTRODUCTION

The body of chemical literature covering the asymmetric synthesis of various organic molecules is vast; however, the purposeful synthesis of transition metal octahedral complexes with defined optical stereochemistry at the metal center (Λ or Δ) has not received nearly as much attention. When considering tris-chelated metal complexes, either homo- or heteroleptic, a common method to generate separate optical isomers is via the resolution of the more easily synthesized racemic mixtures using techniques such as spontaneous resolution, preferential crystallization, chiral column chromatography or coordination and precipitation using chiral counterions.[1] The more difficult route is to synthesize the appropriate optical isomer directly from an achiral metal complex. One way of achieving this is through chirality transfer (or chiral induction) whereby a chiral ligand induces chirality at the metal center upon coordination. This technique has been around for some time, certainly since the early work of Smirnoff on Pt(IV) complexes of (*S*)- and (*R*)-1,2-diaminopropane in 1926,[2] but has not been fully exploited until recently by the groundbreaking work of von Zelewsky[3] and the subsequent clever work on chiral auxiliaries by Meggers and co-workers.[4] In addition to the extensive articles by these two authors, the extension of the chiral induction technique to generate inorganic chiral catalysts, magnets, switches, liquid crystals, polymers, helicates, and extended supramolecular arrays is now a very active area of research.[5]

Our entry into this area of research came about somewhat accidentally during our investigation of the synthesis and reactivity of valent-averaged diruthenium(II,III) tetracarboxylate adducts, $[Ru_2(\mu\text{-}O_2CR)_4L_2](PF_6)$, where L = Lewis base and R = alkyl, aryl, metallocenyl group. We noticed that the reaction of the diruthenium(II,III) tetracarboxylate core with *achiral* phosphines and diphosphines led to a disassembly reaction. In short, diphosphines initially bind to the kinetically favored axial positions on the diruthenium, followed by a slower migration to the more thermodynamically favored equatorial positions (where there is greater π electron density from the metals) with concomitant displacement of some of the bridging carboxylates as well as an intramolecular (carboxylate-bridge induced) reduction. The metal−metal bond is compromised, cleaves, and two molar equivalents of a monocarboxylato-bis-diphosphino-Ru(II) complex are generated. (A more detailed description is given in ref 6.) While these mononuclear Ru(II) complexes can certainly be prepared from mononuclear starting

Received: July 23, 2013
Published: September 10, 2013

   dx.doi.org/10.1021/ic401908t | *Inorg. Chem.* 2013, 52, 11563−11572

materials, the yields of complexes, particularly ones containing bulky R groups, are significantly higher (>80% vs 60%)[6] using this *disassembly* methodology since there is more space around the dimer starting material initially to accommodate the bulkier carboxylate R group; i.e., it is already "in place" (coordinated) and does not have to experience the steric challenge of "getting into place" (coordinating) onto the mononuclear starting material.

In an earlier communication in this journal, we reported on the reaction of the diruthenium(II,III) tetraacetate core with the *chiral* diphosphines *R,R*- and *S,S*-Chiraphos (see ligand structures in Chart 1), which through chiral induction led to

Chart 1. Chiral Diphosphine Ligands[a]

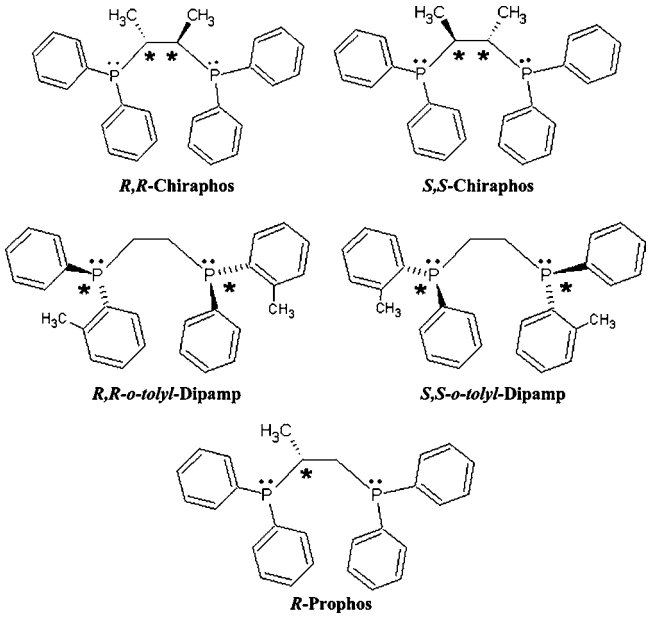

[a]Asterisk (*) = chiral center.

the complexes Λ-[Ru(η^2-O_2CCH_3)(η^2-*R,R*-Chiraphos)$_2$](PF$_6$), and Δ-[Ru(η^2-O_2CCH_3)(η^2-*S,S*-Chiraphos)$_2$](PF$_6$), respectively, with very high diastereoselectivity.[7] We extend this work here to study the effect on the chiral induction process of (a) changing the carboxylate R group from -CH_3 to -C_6H_5, (b) moving the chiral center(s) from the spacer ethylene group in Chiraphos to the coordinating phosphorus atoms in the Dipamp ligands, and (c) reducing the number of chiral centers from 2 to 1 in the ligand Prophos.

2. EXPERIMENTAL SECTION

2.1. General. All synthetic procedures were carried out in an argon atmosphere. The starting materials, [$Ru_2(\mu$-$O_2CCH_3)_4(H_2O)_2$](PF$_6$) and $Ru_2(\mu$-$O_2CC_6H_5)_4$Cl, were prepared using known literature preparations[8] and 1,2-bis(diphenylphosphino)ethane (dppe), 2*R*,3*R*-(+)-bis(diphenylphosphino)butane (*R,R*-Chiraphos), 2*S*,3*S*-(−)-bis-(diphenylphosphino)butane (*S,S*-Chiraphos), 2*R*-(+)-bis-(diphenylphosphino)propane (*R*-Prophos), 1*R*,2*R*-(+)-bis-((*o*-tolyl)-(diphenylphosphino))-ethane (*R,R*-*o*-tolyl-Dipamp), and 1*S*,2*S*-bis-(−)-((*o*-tolyl)(diphenylphosphino))ethane (*S,S*-*o*-tolyl-Dipamp) were used as received from the supplier. **(Note that *S*-Prophos was not available from any known supplier).** IR spectra were recorded as KBr discs on a Varian 640 FTIR spectrometer and ^{31}P NMR spectra on a Bruker Avance 400 MHz spectrometer. UV−vis spectra were measured on a Varian Cary 100 spectrophotometer using matched Hellma 1 cm quartz cuvettes or together with the circular dichroism (CD) spectra on a Jasco J-815 CD spectrophotometer. (Solution spectra were run in $CHCl_3$ at concentrations in the range of 2.0×10^{-5} to 1.0×10^{-4} M. Solid state spectra were run as KBr discs). All elemental analyses were carried out by Canadian Microanalytical Service Ltd., Delta, BC. Please see Discussion, section 3.2.3 for the reason why complexes **IV** and **V** are designated with commas.

2.2. Syntheses. *2.2.1. Bis(methanol)-tetra-μ-benzoato(O,O′)-diruthenium(II,III) Hexafluorophosphate, [$Ru_2(\mu$-$O_2CC_6H_5)_4(MeOH)_2$](PF$_6$), **I**.* This complex was prepared in a similar fashion to the ferrocenoato derivatives that Cooke et al. prepared.[9] $Ru_2(\mu$-$O_2CC_6H_5)_4$Cl (0.150 g, 0.208 mmol) was placed in an Erlenmeyer flask, shielded from light, and dissolved in 20 mL of methanol with low heat (40−50 °C) and stirring. $AgPF_6$ (0.052 g, 0.208 mmol) was added, and the solution was refluxed for 12 h. The solution was then filtered over Celite, and the solvent was removed under reduced pressure. The crude product was recrystallized once from methanol and used without further purification or extensive characterization. Yield = 0.180 g (0.201 mmol), 97%. $C_{30}H_{28}F_6O_{10}PRu_2$ (895.65): calculated C 40.23, H 3.15; found C 40.41, H 3.02. IR (cm^{-1}): 3528 (m), 3068 (w), 1601 (s), 1497 (s), 1465 (s), 1403 (s), 1254 (w), 1181 (m), 1145 (m), 1072 (w), 1027 (m), 845 (s), 716 (s), 691 (s), 560 (s), 536 (s).

*2.2.2. Δ,Λ-(Benzoato-O,O′)-bis(1,2-bis(diphenylphosphino)-ethane-P,P′)ruthenium(II) Hexafluorophosphate, [Δ,Λ-Ru(η^2-$O_2CC_6H_5$)(η^2-dppe)$_2$](PF$_6$), **II**.* Complex **I** (0.080 g, 0.089 mmol) was dissolved, with mild heating and stirring, in 150 mL of previously degassed methanol over a period of 1−2 h. Dppe (0.142 g, 0.356 mmol) was dissolved with mild heat and stirring in 50 mL of previously degassed methanol and then added to the complex **I** solution. Upon combining of the solutions, the golden color darkened to a deep brown. The reaction was allowed to reflux under argon for 12 h. After about 6 h, the solution lightened significantly to a bright yellow. After the reflux was complete, the solution was allowed to cool to room temperature, and 0.015 g (0.089 mmol) of NH_4PF_6 was added. The volume was reduced to 30 mL under reduced pressure and cooled at 4° overnight to yield pale yellow needlelike crystals that can be washed with ice cold methanol. Crystallization from methanol yielded 0.193 g, 0.166 mmol (93%). $C_{59}H_{53}F_6O_2P_5Ru$ (1164.00): calculated C 60.88, H 4.59, P 13.30; found C 61.15, H 4.69, P 13.53. IR (cm^{-1}): 3057 (w), 2930 (w), 1500 (m), 1485 (m), 1434 (s), 1384 (m), 1099 (m), 1000 (w), 839 (s), 747 (m), 698 (s), 558 (m), 528 (s). ^{31}P NMR in $CDCl_3$ (δ/ppm): −144.33 (septet, 1 P), 58.81 (triplet, 2 P), 63.66 (triplet, 2 P), J_{P-P} = 21.2 Hz. UV−vis in $CHCl_3$ (λ_{max}/nm (ε/M^{-1} cm^{-1})): 235 (60800), 262 (48600), 360 (2070), 390sh (1100).

*2.2.3. Λ-(Benzoato-O,O′)-bis(R,R-1,2-bis(diphenylphosphino)-butane-P,P′)ruthenium(II) Hexafluorophosphate, [Λ-Ru(η^2-$O_2CC_6H_5$)(η^2-R,R-Chiraphos)$_2$](PF$_6$), **Λ-R,R-III**.* Complex **I** (0.080 g, 0.089 mmol) was dissolved in 150 mL of previously degassed methanol with mild heating and stirring for 1 h. *R,R*-Chiraphos (0.152 g, 0.357 mmol) was dissolved in 50 mL of previously degassed methanol and added to the complex **I** solution. The combined solutions were left to reflux under argon for 12 h during which a color change from brown to yellow was observed. The solution was then cooled and NH_4PF_6 (0.015 g, 0.089 mmol) added with stirring. The solution was filtered, concentrated to 40 mL under reduced pressure, and cooled at −10 °C overnight. The crude, bright yellow powder obtained was recrystallized by slow evaporation from methanol or ethanol. Yield: 0.186 g, 0.160 mmol (86%). $C_{63}H_{61}F_6O_2P_5Ru$ (1220.08): calculated C 62.02, H 5.04, P 12.69; found C 62.28, H 5.24, P 12.53. IR (cm^{-1}): 3448 (w), 3057 (w), 2969 (w), 2928 (w), 1501 (w), 1485 (m), 1434 (s), 1384 (m), 1188 (w), 1097 (m), 1026 (w), 840 (s), 745 (m), 700 (m), 656 (w), 609 (m), 557(w), 533 (m), 454 (s). ^{31}P NMR in $CDCl_3$ (δ/ppm): −144.25 (septet, 1 P), 58.60 (triplet, 2P), 63.45 (triplet, 2P), J_{P-P} = 23.5 Hz. UV−visible in $CHCl_3$ (λ_{max}/nm (ε/M^{-1}cm^{-1})): 242 (47400), 264 (56200), 379 (1420). CD in $CHCl_3$ (λ/nm, $\Delta\varepsilon$/M^{-1} cm^{-1}): 320, +25; 370, −40; 435, +23.

*2.2.4. Δ-(Benzoato-O,O′)-bis(S,S-1,2-bis(diphenylphosphino)-butane-P,P′)ruthenium(II) Hexafluorophosphate, [Δ-Ru(η^2-$O_2CC_6H_5$)(η^2-S,S-Chiraphos)$_2$](PF$_6$), **Δ-S,S-III**.* This was prepared and purified in a similar fashion to complex **Λ-R,R-III** except that *S,S*-

dx.doi.org/10.1021/ic401908t | Inorg. Chem. 2013, 52, 11563−11572

Chiraphos was used as the chiral diphosphine. Yield: 0.208 g, 0.169 mmol (95%). $C_{63}H_{61}F_6O_2P_5Ru$ (1220.08): calculated C 62.02, H 5.04, P 12.69; found C 61.95, H 4.91, P 12.89. IR (cm^{-1}): 3447 (w). 3057 (w), 2968 (w), 2928 (w), 1501 (w), 1484 (m), 1434 (s), 1384 (m), 1189 (w), 1097 (w), 1029 (w), 840 (s), 745 (m), 700 (m), 659 (w), 614 (w), 558 (m), 534 (m), 459 (s). ^{31}P NMR in $CDCl_3$ (δ/ppm): −144.25 (septet, 1P), 58.57 (triplet, 2P), 63.47 (triplet, 2P), J_{P-P} = 23.5 Hz. UV−vis in $CHCl_3$ (λ_{max}/nm (ε/M^{-1} cm^{-1})): 242 (47400), 264 (56200), 379 (1420). CD in $CHCl_3$ (λ/nm, $\Delta\varepsilon/M^{-1}cm^{-1}$): 320, −25; 370, +40; 435, −22.

*2.2.5. Δ-(Benzoato-O,O′)-bis(R,R-1,2-bis((o-tolyl)-(phenylyphosphine))ethane-P,P′)ruthenium(II) Hexafluorophosphate, [Δ-Ru(η^2-$O_2CC_6H_5$)(R,R-o-tolyl-Dipamp)$_2$](PF_6), "**Δ-R,R-IV**".* This complex was prepared and purified using a similar procedure as that for **Λ-*R,R*-III** except that *R,R-o*-tolyl-Dipamp (0.152 g, 0.356 mmol) was used. Yield: 0.189 g, 0.155 mmol (87%). $C_{63}H_{61}F_6O_2P_5Ru$ (1220.08): calculated C 62.02, H 5.04, P 12.69; found C 61.88, H 5.14, P 12.76. IR (cm^{-1}): 3055 (w), 2933 (w), 1509 (m), 1433 (s), 1384 (m), 1318 (w), 1279 (w), 1202 (w), 1176 (w), 1104 (w), 1028 (w), 835 (s), 750 (m), 721 (m), 706 (s), 685 (m), 652 (w), 556 (s), 528 (s), 512 (m), 463 (m). ^{31}P NMR in $CDCl_3$ (δ/ppm): −144.31 (septet, 1 P), 58.59 (triplet, 2 P), 69.80 (triplet, 2 P), J_{P-P} = 18.7 Hz. UV−vis in $CHCl_3$ (λ_{max}/nm (ε/M^{-1} cm^{-1})): 239 (49600), 258 (58100), 375 (1360). CD in $CHCl_3$ (λ/nm, $\Delta\varepsilon/M^{-1}$ cm^{-1}): 316, −51; 364, +59; 402, −25; 448, +2.

*2.2.6. Λ-(Benzoato-O,O′)-bis(S,S-1,2-bis((o-tolyl)-(phenylyphosphine))ethane-P,P′)ruthenium(II) hexafluorophosphate, [Λ-Ru(η^2-$O_2C_6CH_5$)(S,S-o-tolyl-dipamp)$_2$](PF_6), "**Λ-S,S-IV**".* This complex was prepared and purified using a similar procedure as that for **Λ-*R,R*-III** except that *S,S-o*-tolyl-Dipamp (0.220 g, 0.517 mmol) was used. Yield: 0.183 g, 0.150 mmol (85%). $C_{63}H_{61}F_6O_2P_5Ru$ (1220.08): calculated C 62.02, H 5.04, P 12.69; found C 62.05, H 5.10, P 12.54. IR (cm^{-1}): 3055 (w), 2934 (w), 1510 (m), 1434 (s), 1384 (m), 1318 (w), 1279 (w), 1202 (w), 1176 (w), 1104 (w), 1068 (w), 1028 (w), 835 (s), 750 (m), 721 (m), 706 (s), 652 (w), 556 (s), 528 (s), 512 (m), 463 (m). ^{31}P NMR in $CDCl_3$ (δ/ppm): −144.30 (septet, 1 P), 58.59 (triplet, 2 P), 69.83 (triplet, 2 P), J_{P-P} = 18.7 Hz . UV−vis in $CHCl_3$ (λ_{max}/nm (ε/M^{-1} cm^{-1})): 239 (49600), 258 (58100), 375 (1360). CD in $CHCl_3$ (λ/nm, $\Delta\varepsilon/M^{-1}$ cm^{-1}): 316, +50; 364, −57; 402, +25; 448, −3.

*2.2.7. Δ-(Acetato-O,O′)-bis(R,R-1,2-bis((o-tolyl)-(phenylyphosphine))ethane-P,P′)ruthenium(II) Hexafluorophosphate, [Δ-Ru(η^2-O_2CCH_3)(R,R-o-tolyl-dipamp)$_2$](PF_6), "**Δ-R,R-V**".* $[Ru_2(\mu\text{-}O_2CCH_3)_4(H_2O)_2](PF_6)$ (0.080 g, 0.129 mmol) was dissolved in 10 mL of previously degassed methanol and added to *R,R-o*-tolyl-Dipamp (0.220 g, 0.517 mmol) dissolved in 200 mL of degassed methanol. The resulting dark red solution was allowed to reflux under argon for 8 h over which time the color gradually changed to bright yellow. The reaction was allowed to cool and NH_4PF_6 (0.021 g, 0.129 mmol) was added with stirring. The volume of the solution was reduced to 20 mL via rotary evaporation and cooled at 4 °C overnight. The yellow product was collected by suction filtration and with a minimal amount of ice-cold methanol. Yield: 0.252 g, 0.218 mmol (84%). $C_{58}H_{59}F_6O_2P_5Ru$ (1158.02): calculated C 60.16, H 5.14, P 13.37; found C 59.81, H 5.09, P 13.12. IR (cm^{-1}): 3446 (w), 3056 (w), 2928 (w), 1469 (m), 1436 (m), 1282 (w), 1200 (w), 1096 (w), 840 (s), 748 (m), 698 (m), 617 (w), 558 (m), 536 (m), 503 (w), 451 (w). ^{31}P NMR in $CDCl_3$ (δ/ppm): −144.29 (septet, 1 P), 34.67 (triplet, 2 P), 57.77 (triplet, 2 P), J_{P-P} = 14.6 Hz. UV−vis in $CHCl_3$ (λ_{max}/nm (ε/M^{-1} cm^{-1})): 237 (46500), 248 (56200), 355 (2150), 403sh (1460) CD in $CHCl_3$ (λ/nm, $\Delta\varepsilon/M^{-1}$ cm^{-1}): 312, −73; 359, +101; 396, −57; 441, +9.

*2.2.8. Λ-(Acetato-O,O′)-bis(S,S-1,2-bis((o-tolyl)-(phenylyphosphine))ethane-P,P′)ruthenium(II) Hexafluorophosphate, [Λ-Ru(η^2-O_2CCH_3)(S,S-o-tolyl-dipamp)$_2$](PF_6), "**Λ-S,S-V**".* This complex was prepared and purified using a similar procedure as that for "**Δ-*R,R*-V**" except that *S,S-o*-tolyl-Dipamp (0.220 g, 0.517 mmol) was used. Yield: 0.266 g, 0.229 mmol (89%). $C_{58}H_{59}F_6O_2P_5Ru$ (1158.02): calculated C 60.16, H 5.14, P 13.37; found C 59.78, H 5.15, P 13.77. IR (cm^{-1}): 3434 (w), 3057 (w), 2930 (w), 1468 (m), 1437 (m), 1285 (w), 1181 (w), 1097 (w), 1036 (w), 998 (w), 841 (s), 748 (m), 698 (m), 616 (w), 558 (m), 537 (m), 503 (w), 451 (w). ^{31}P NMR in $CDCl_3$ (δ/ppm): −144.30 (septet, 1 P), 34.50 (triplet, 2 P), 57.79 (triplet, 2 P), J = 14.6 Hz. UV−vis in $CHCl_3$ (λ_{max}/nm (ε/M^{-1} cm^{-1})): 237 (46500), 248 (56200), 355 (2150), 403sh (1460). CD in $CHCl_3$ (λ/nm, $\Delta\varepsilon/M^{-1}$ cm^{-1}): 312, +73; 359, −99; 396, +57; 441, −10.

*2.2.9. Λ-(Acetato-O,O′)-bis(R-1,2-bis(diphenylphosphino)-propane-P,P′)ruthenium(II) Hexafluorophosphate, [Λ-Ru(η^2-O_2CCH_3)(R-Prophos)$_2$](PF_6), **Λ-*R,R*-VI**.* This complex was prepared and purified using a similar procedure as that for "**Δ-*R,R*-V**" except that *R*-Prophos (0.196 g, 0.476 mmol) was used. Crystals suitable for X-ray diffraction were grown by diffusion of diethyl ether into a 1,2-dichloroethane solution of the product. Yield: 0.211 g, 0.668 mmol (79%). $C_{56}H_{33}F_6O_2P_5Ru$ (1129.98 g mol^{-1}): calculated C 59.52, H 4.91, P 13.71; found C 59.31, H 5.02, P 13.89%. IR (cm^{-1}): 3430 (w), 3059 (w), 2934 (w), 1469 (m), 1441 (m), 1102 (m), 998 (w), 844 (s), 744 (m), 698 (m), 626 (w), 605 (w), 555 (m), 523 (s). ^{31}P NMR in $CDCl_3$ (δ/ppm): −144.28 (septet, 1P), 44.29 (triplet, 2P), 65.67 (triplet, 2P), J_{P-P} = 20.4 Hz. UV−visible in $CHCl_3$ (λ_{max}/nm($\varepsilon/M^{-1}cm^{-1}$): 238 (48700), 246 (55800), 382 (1400). CD in $CHCl_3$ (λ/nm, $\Delta\varepsilon/M^{-1}$ cm^{-1}): 311, +43; 352, −57; 392, +44.

2.3. X-ray Crystallography. X-ray structures were determined for complexes **II·MeOH**, **Λ-*R,R*-III·2.75 EtOH**, **Δ-*S,S*-III·1.875 MeOH**, "**Δ-*R,R*-IV**", "**Λ-*S,S*-IV**", and **Λ-*R*-VI** using a Bruker SMART APEX II X-ray diffractometer with graphite monochromated Mo Kα radiation (λ = 0.71073 Å), operating at 50 kV and 30 mA over 2θ ranges of 2.24−4.10 to 52.00°. The data were collected and processed on a PC using the Bruker AXS Crystal Analysis Package.[10] Neutral atom scattering factors were taken from Cromer and Waber.[11] All hydrogen atoms were refined anisotropically. All H atoms were placed in geometrically calculated positions, with C−H = 0.95 (aromatic), 0.98(CH_3), 0.99(CH_2) Å, and 1.00 Å (aliphatic CH), and refined as riding atoms, with U_{iso}(H) = 1.5U_{eq}C(CH_3) or 1.2U_{eq}C (other C). For **II**, the methanol of solvation and one of the two DPPE ligands were disordered. For **Λ-*R,R*-III**, difference electron density maps revealed the presence of disordered PF_6^- and lattice ethanol molecules, which were ultimately modeled through the use of the SQUEEZE subroutine of the PLATON software suite.[12] (Please note that use of the SQUEEZE subroutine leads to occasional ALERT A warnings in the CheckCif program; these can be ignored.) Two smaller voids and one large void per lattice were found. Each smaller void comprises a total volume of 341 Å^3 and contributes a total of 138 electrons, and the large void has a doubled volume and electrons. Each smaller void was thus assigned to one disordered PF_6^- and 2.5 EtOH, which contributes 70 + 65 = 135 electrons and occupies about 290 Å^3 in space. The large void was assigned to two PF_6^- and 6 EtOH molecules, which contributes 70 × 2 + 6 × 26 = 296 electrons and occupies about 640 Å^3 in space. The larger volume of the void may be a result of the disorder. The contributions have been included in all derived crystal quantities. For **Δ-*S,S*-III**, the difference electron density maps revealed the presence of disordered PF_6^- and lattice methanol molecules, which were modeled through the use of the SQUEEZE subroutine of the PLATON software suite as for **Λ-*R,R*-III** above. Two smaller voids and one large void per lattice were found. Each smaller void comprises a total volume of 249 Å^3 and contributes a total of 97 or 98 electrons, and the large void has a doubled volume but more than doubled electrons. Each smaller void was thus assigned to one disordered PF_6^- and 1.5 MeOH, which contributes 70 + 27 = 97 electrons, and occupies about 200 Å^3 in space. The large void was assigned to two PF_6^- and 4.5 MeOH molecules, which contributes 70 × 2 + 4.5 × 18 = 221 electrons and occupies about 460 Å^3 in space. The larger volume of the void may be a result of the disorder. The contributions have been included in all derived crystal quantities. For "**Δ-*R,R*-IV**", only one H atom on benzoate (H33a) was located from difference Fourier map, and all the other H atoms were placed in geometrically calculated positions as mentioned above. For "**Λ-*S,S*-IV**", only one H atom on benzoate (H33a) was located from difference Fourier map, and all the other H atoms were placed in geometrically calculated positions as mentioned above. For **Λ-*R*-VI**, the methyl groups were refined with AFIX 137, which allowed the rotation of the methyl groups while

Table 1. Crystal Data and Structure Refinement Parameters

	II·MeOH	Δ-*S,S*-III·1.875 MeOH	Λ-*R,R*-III·2.75 EtOH	"Λ-*S,S*-IV"	"Δ-*R,R*-IV"	Λ-*R*-VI
empirical formula	$C_{60}H_{57}F_6O_3P_5Ru$	$C_{64.88}H_{8.5}F_6O_{3.88}P_5Ru$	$C_{68.5}H_{77.5}F_6O_{4.75}P_5Ru$	$C_{63}H_{61}F_6O_2P_5Ru$	$C_{63}H_{61}F_6O_2P_5Ru$	$C_{56}H_{55}F_6O_2P_5Ru$
M/g·mol^{-1}	1195.98	1280.12	1346.72	1220.04	1220.04	1129.92
crystal size/mm	0.10 × 0.04 × 0.04	0.15 × 0.10 × 0.08	0.10 × 0.06 × 0.06	0.20 × 0.15 × 0.08	0.25 × 0.25 × 0.15	0.20 × 0.15 × 0.08
2θ range/deg	2.24−52.00	2.60−52.00	3.40−52.00	3.48−52.00	3.48−52.00	4.10−52.00
h; k; l; range	±30; ±15; ±45	±14; ±28; ±26	±14; −28,25; ±26	±17; −24,22; −21,23	−17,11; −22,24; ± 23	±13; −18,24; −9,15
crystal system	monoclinic	monoclinic	monoclinic	orthorhombic	orthorhombic	monoclinic
space group	$C2/c$	$P2_1$	$P2_1$	$C222_1$	$C222_1$	$P2_1$
a/Å	24.472(7)	12.0349(1)	12.0896(5)	14.3933(3)	14.3816(3)	11.3239(2)
b/Å	12.277(3)	23.159(3)	23.3404(12)	20.0890(4)	20.1066(3)	19.5588(4)
c/Å	37.226(10)	21.5330(3)	21.6023(11)	19.2867(4)	19.2514(3)	12.8717(4)
α/deg	90	90	90	90	90	90
β/deg	103.418(4)	97.339(1)	97.579(3)	90	90	116.0880(10)
γ/deg	90	90	90	90	90	90
V/Å^3	10879(5)	5952.46(12)	6042.4(5)	5576.7(2)	5566.83(17)	2560.40(11)
Z	8	4	4	4	4	2
D_{calc}/g cm^{-3}	1.460	1.428	1.480	1.453	1.456	1.466
F (000)	4912	2647	2798	2512	2512	1160
μ/mm^{-1}	0.502	0.465	0.463	0.490	0.491	0.527
max/min trans	0.9802/0.9515	0.9638/0.9336	0.9728/0.9552	0.9619/0.9084	0.9301/0.8872	0.9591/0.9020
reflec collected	53512	63929	58831	15465	24345	14248
indep refl (R_{int})	10681 (0.2214)	23023 (0.0356)	19271 (0.1362)	5484 (0.0315)	5438 (0.0239)	8708 (0.0261)
obs refl [$I > 2\sigma(I)$]	4932	19353	10481	5171	5309	7275
parameters refined	620	1263	1261	355	355	647
max/min $\Delta\rho^a$/e Å^{-3}	0.744/−0.647	0.348/−0.323	1.810/−1.035	0.701/−0.283	0.369/−0.263	0.631/−0.461
R_1/wR_2 [$I > 2\sigma(I)$]^b	0.0766/0.1545	0.0315/0.0667	0.0703/0.1421	0.0287/0.0669	0.0202/0.0511	0.0423/0.0819
R_1/wR_2 (all refl)^b	0.1869/0.2101	0.0402/0.0697	0.1243/0.1625	0.0310/0.0681	0.0210/0.0516	0.0580/0.0889
GOF on F^{2c}	1.002	0.995	0.905	1.031	1.064	1.020
Flack parameter^d	N/A	0.012(11)	0.00(3)	0.07(2)	−0.009(16)	−0.04(3)

^{a}Largest difference peak and hole. $^b R_1 = \Sigma||F_o| - |F_c||/\Sigma|F_o|$; $wR_2 = [\Sigma w(F_o^2 - F_c^2)^2/\Sigma w(F_o^2)^2]^{1/2}$. ^{c}GOF = $[\Sigma[w(F_o^2 - F_c^2)^2]/(n-p)]^{1/2}$. ^{d}Absolute structure parameter.

keeping the C−H distances and X−C−H angles fixed. The PF_6^- anion is disordered.

3. RESULTS AND DISCUSSION

3.1. Synthesis and Preliminary Characterization. Synthesis of the desired complexes was relatively straightforward following previously documented preparations. $Ru_2(\mu\text{-}O_2CC_6H_5)_4Cl$ is readily prepared by a carboxylate exchange reaction from $Ru_2(\mu\text{-}O_2CCH_3)_4Cl$.[8b] Both of these complexes can then be dechlorinated in methanol with $AgPF_6$ to generate the more useful diadducts, $[Ru_2(\mu\text{-}O_2CR)_4(MeOH)_2](PF_6)$ R = CH_3 or C_6H_5 (**I**). Subsequent reaction of either the acetate or benzoate diadduct with the appropriate chiral (or achiral) diphosphine yielded the desired products. A detailed outline of the mechanism of this reaction is reported elsewhere,[6] and a discussion of the possibility of any epimerization processes is given in our earlier communication.[7] The benzoate diadduct yielded the Ru(II) complexes $[Ru(\eta^2\text{-}O_2CC_6H_5)(\eta^2\text{-dppe})_2](PF_6)$ **II**, Λ-$[Ru(\eta^2\text{-}O_2CC_6H_5)(\eta^2\text{-}R,R\text{-Chiraphos})_2](PF_6)$ **Λ-*R,R*-III**, Δ-$[Ru(\eta^2\text{-}O_2CC_6H_5)(\eta^2\text{-}S,S\text{-Chiraphos})_2](PF_6)$ **Δ-*S,S*-III**, Λ-$[Ru(\eta^2\text{-}O_2CC_6H_5)(\eta^2\text{-}S,S\text{-}o\text{-}tolyl\text{-Dipamp})_2](PF_6)$ "**Λ-*S,S*-IV**", and Δ-$[Ru(\eta^2\text{-}O_2CC_6H_5)(\eta^2\text{-}R,R\text{-}o\text{-}tolyl\text{-Dipamp})_2](PF_6)$ "**Δ-*R,R*-IV**", whereas the acetate diadduct was converted to Λ-$[Ru(\eta^2\text{-}O_2CCH_3)(\eta^2\text{-}S,S\text{-}o\text{-}tolyl\text{-Dipamp})_2](PF_6)$ "**Λ-*S,S*-V**", Δ-$[Ru(\eta^2\text{-}O_2CCH_3)(\eta^2\text{-}R,R\text{-}o\text{-}tolyl\text{-Dipamp})_2](PF_6)$ "**Δ-*R,R*-V**", and Λ-$[Ru(\eta^2\text{-}O_2CCH_3)(\eta^2\text{-}R\text{-Prophos})_2](PF_6)$ **Λ-*R*-VI**. All complexes gave satisfactory elemental analyses.

The infrared spectra of all the mononuclear Ru(II) complexes resemble those of the achiral analogues such as $[Ru(\eta^2\text{-}O_2CCH_3)(\eta^2\text{-dppe})_2](PF_6)$.[6a] For example, the symmetric and asymmetric carboxylate stretches, $\nu_{sym}(COO)$ and $\nu_{asym}(COO)$, are found in the range 1433−1510 cm^{-1} with $\nu_{asym}(COO) - \nu_{sym}(COO) = 28-76$ cm^{-1}, indicative of the η^2 binding mode.[13] A strong band is also seen at around 840 cm^{-1} due to the ν(P−F) of the PF_6^- counterion.[13]

^{31}P NMR spectra in chloroform have been found to be very diagnostic for complexes of the type, $[Ru(\eta^2\text{-}O_2CR)(\eta^2\text{-dppe})_2](PF_6)$ (R = Me, ferrocenyl or ruthenocenyl) where a five-membered ring is formed between the diphosphine ligand and the metal,[14] and these have been thoroughly assigned previously.[6a] For example, $[Ru(\eta^2\text{-}O_2CCH_3)(\eta^2\text{-dppe})_2](PF_6)$ displays a doublet of triplets at 55.32 ppm (due to the two equivalent P's bound trans to O) and 57.02 ppm (2 P's bound trans to P), and J_{PP} = 18.1 Hz (A_2B_2 or A_2X_2 spin system). As well, a septet is seen at −146.5 ppm due to the P−F coupling of the PF_6^- counterion. In all of the complexes studied here, where only five-membered rings are formed, a similar pattern emerges. (Data are included in the Experimental Section.) Septets for the PF_6^- counterion are seen around −144.3 ppm, and in all cases for the pure products in solution a pair of triplets are seen in the range 34.50−69.83 ppm. Values are essentially identical for enantiomeric pairs, and no peaks due to

dx.doi.org/10.1021/ic401908t | Inorg. Chem. 2013, 52, 11563−11572

the presence of any diastereomers are seen. (A typical spectrum is shown in Figure S1 of the Supporting Information.) It should be noted that complex **Λ-*R*-VI** has the potential of four different binding modes for the two *R*-Prophos ligands (i.e., methyl group on each ligand, adjacent to P bound trans to O for both diphosphines; methyl group on each ligand, adjacent to P bound trans to P for both diphosphines; and one diphosphine binding one way and the other the opposite way, which will not be exactly identical because of the chirality at the metal center). In the crude reaction product all of these peaks are seen (see Figure S4 in the Supporting Information which shows eight triplets albeit six of which are quite weak); however the signals due to the *R*-Prophos ligands bound with the methyl groups adjacent to the P's bound *trans* to O are by far the predominant ones, and the minor peaks disappear completely upon recrystallization. (This is confirmed by the crystal structure below.) As with the other complexes, there is no evidence in the NMR of the diastereomer which in this case would be **Δ-*R*-VI**.

As seen for $[Ru(\eta^2\text{-}O_2CCH_3)(\eta^2\text{-dppe})_2](PF_6)$,[6a] electronic spectra show the characteristic $\pi^* \leftarrow \pi$ (ligand-based ct) and lmct (Ru(II) ← phosphine/carboxylate) bands in the range 200−300 nm, as well as an mlct (P ← Ru(II)) between 310 and 400 nm and d−d transitions >360 nm (normally buried under the mlct). (A representative spectrum is given in the Supporting Information.)

3.2. X-ray Crystallography and Circular Dichroism. Crystals suitable for X-ray diffraction were grown from methanol or ethanol for all of the complexes except "**Λ-*S,S*-V**" and "**Δ-*R,R*-V**" and in the those cases where a particular diastereomer was formed (**III**, **IV**, and **VI**), structures were determined on 5−8 separate crystals from 2 to 3 separate reaction batches. In all cases, identical structures of the same diastereomer were obtained. Crystal and refinement data are given in Table 1. The bond lengths and angles around the distorted octahedral Ru(II) core are similar to those seen in previous complexes of the type, $[Ru(\eta^2\text{-}O_2CR)(\eta^2\text{-diphosphine})](PF_6)$,[6] and selected ones are given in the figure captions of each structure (see below). It should be noted that in all cases the Ru−P bond trans to O is significantly shorter than the Ru−P bond trans to P; indicating a strong trans influence, as expected.

Circular dichroism spectra were run for all complexes both in solution ($CHCl_3$) and in the solid-state as KBr discs. For those complexes where single crystals were obtained, a solid-state CD spectrum was run on the crystals of known stereochemistry (from the X-ray analysis) followed by a CD spectrum of the bulk solid and found to be identical. From this we can conclude that the bulk solid had predominantly (essentially exclusively) the same stereochemistry as those crystals for which structures were determined. Likewise for the solution measurements, single crystals of known structure were found to give identical spectra to those of the bulk sample, and the solution spectra were also found to be similar to the solid-state spectra indicating the same predominant form exists in both phases. In all cases, the CD signal for the free ligands lie below 290 nm.[15] As well, none of the solution CD signals changed over a period of at least 5 days at room temperature, supporting our earlier conclusion[7] that the rate of epimerization at the relatively inert Ru(II) centers is quite slow if it occurs at all. Let us now deal with each complex (or pair of complexes) in a bit more detail.

*3.2.1. [Δ,Λ-Ru(η²-O₂CC₆H₅)(η²-dppe)₂](PF₆), **II·MeOH**.* Introducing the bulkier R group (phenyl vs methyl) changes little in the overall physical properties of the racemic derivative, $[\Delta,\Lambda\text{-}Ru(\eta^2\text{-}O_2CC_6H_5)(\eta^2\text{-dppe})_2](PF_6)$, **II**. It crystallizes with a methanol of solvation in the nonchiral monoclinic space group, *C*2/*c*, and contains a racemic mixture of Δ and Λ forms. The molecular structure (including selected bond lengths and angles) can be seen in Figure 1. The CD spectrum of **II** displays no signal in the range 290−550 nm.

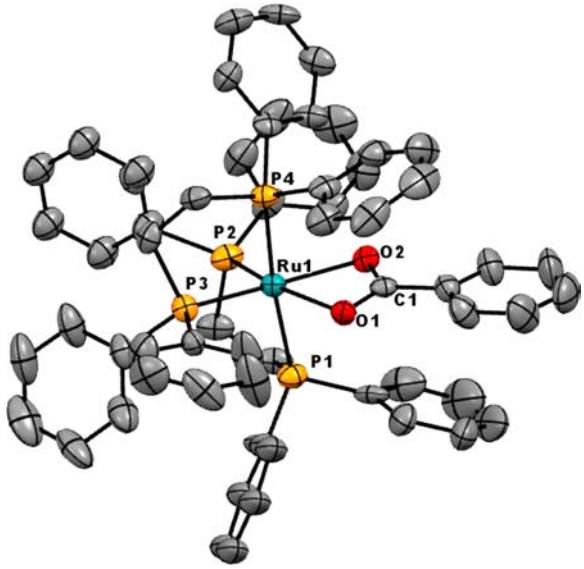

Figure 1. Molecular structure of $\mathbf{II}^+$. Hydrogen atoms, methanol of solvation and PF_6^- ions omitted for clarity. Selected bond lengths (Å) and angles (°): Ru(1)−O(1) 2.169(5), Ru(1)−O(2) 2.184 (5), Ru(1)−P(1) 2.366(2), Ru(1)−P(2) 2.306(2), Ru(1)−P(3) 2.296(2), Ru(1)−P(4) 2.373(2); O(1)−Ru(1)−O(2) 60.03(18), P(1)−Ru(1)−P(2) 84.26(8), P(3)−Ru(1)−P(4) 82.73(8), O(1)−Ru(1)−P(1) 85.64(14), O(2)−Ru(1)−P(4) 86.87(13), P(1)−Ru(1)−P(3) 100.63(8), P(2)−Ru(1)−P(4) 101.68(8).

*3.2.2. [Λ-Ru(η²-O₂CC₆H₅)(η²-R,R-Chiraphos)₂](PF₆), **Λ-R,R-III·2.75 EtOH**, and [Δ-Ru(η²-O₂CC₆H₅)(η²-S,S-Chiraphos)₂](PF₆), **Δ-S,S-III·1.875 MeOH**.* In our preliminary Communication,[7] *R,R*- and *S,S*-Chiraphos ligands induced Λ and Δ chirality, respectively, when reacted with $[Ru_2(\mu\text{-}O_2CCH_3)_4(MeOH)_2](PF_6)$ to form $\Lambda\text{-}[Ru(\eta^2\text{-}O_2CCH_3)(\eta^2\text{-}R,R\text{-Chiraphos})_2](PF_6)$ and $\Delta\text{-}[Ru(\eta^2\text{-}O_2CCH_3)(\eta^2\text{-}S,S\text{-Chiraphos})_2](PF_6)$. When we introduce the larger phenyl R-group into the starting dimer, a similar disassembly takes place in this study, and the products have the same stereochemistry; i.e., *R,R*-Chiraphos induces Λ chirality at the metal to form **Λ-*R,R*-III**, and *S,S*-Chiraphos induces Δ chirality to form **Δ-*S,S*-III**. In both cases, the ligands retain their *R,R* and *S,S* stereochemistry. The absolute configurations are confirmed in the X-ray structures of these two complexes as seen in Figure 2 (selected bond lengths and angles are given in the figure caption). The Flack parameters[16] are 0.00(3) for **Λ-*R,R*-III·2.75 EtOH** and 0.012(11) for **Δ-*S,S*-III·1.875 MeOH**. The complexes crystallize in the chiral monoclinic space group, $P2_1$, and contain two unique molecules in the unit cell. The Δ form contains 1.875 molecules of methanol, and the Λ form has 1.75 molecules of ethanol of solvation. The molecules of solvation seen in these two structures are also seen in the ^1H NMR (see, for example, the ^1H NMR spectrum of complex **Λ-*R,R*-III·2.75 EtOH** in Figure S5 in the Supporting Information). The two molecules of the Δ form are not *exact* enantiomers to the two

dx.doi.org/10.1021/ic401908t | *Inorg. Chem.* 2013, 52, 11563−11572

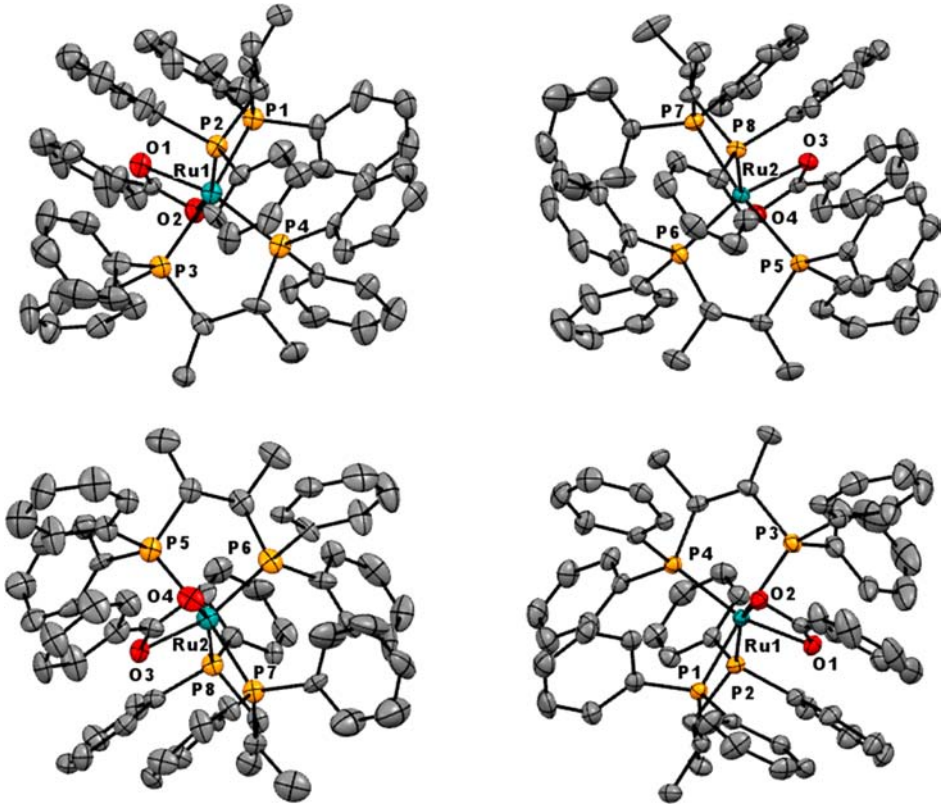

Figure 2. Molecular structure of $[\Lambda\text{-}R,R\text{-III}]^+$ (left) and $[\Delta\text{-}S,S\text{-III}]^+$ (right) showing both unique molecules in the unit cell. Hydrogen atoms, molecules of solvation and PF_6^- ions are omitted for clarity. Selected bond lengths (Å) and angles (°) for $[\Lambda\text{-}R,R\text{-III}]^+$: Ru(1)−O(1) 2.176(6), Ru(1)−O(2) 2.191(5), Ru(1)−P(1) 2.381(2), Ru(1)−P(2) 2.312(2), Ru(1)−P(3) 2.391(2), Ru(1)−P(4) 2.314(3), Ru2−O(3) 2.182(6), Ru(2)−O(4) 2.202(5), Ru(2)−P(5) 2.369(3), Ru(2)−P(6) 2.301(3), Ru(1)−P(7) 2.406(3), Ru(2)−P(8) 2.301(2); O(1)−Ru(1)−O(2) 60.1(2), P(1)−Ru(1)−P(2) 103.75(16), P(3)−Ru(1)−P(4) 83.60(10), O(3)−Ru(2)−O(4) 59.8(2), P(5)−Ru(2)−P(6) 83.69(9), P(7)−Ru(2)−P(8) 84.05(8). For $[\Delta\text{-}S,S\text{-III}]^+$: Ru(1)−O(1) 2.1680(18), Ru(1)−O(2) 2.1955(17), Ru(1)−P(1) 2.3813(7), Ru(1)−P(2) 2.3136(7), Ru(1)−P(3) 2.4005(8), Ru(1)−P(4) 2.3077(7), Ru(2)−O(3) 2.1685(18), Ru(2)−O(4) 2.1873(17), Ru(2)−P(5) 2.3775(8), Ru(2)−P(6) 2.3084(8), Ru(2)−P(7) 2.4137(7), Ru(2)−P(8) 2.3021(6); O(1)−Ru(1)−O(2) 59.70(7), P(1)−Ru(1)−P(2) 83.68(2), P(3)−Ru(1)−P(4) 83.49(3), O(3)−Ru(2)−O(4) 60.17(6), P(5)−Ru(2)−P(6) 83.69(3), P(7)−Ru(2)−P(8) 83.89(3).

molecules of Λ form in the solid state. They are quite close as can be seen in the figure, but because of the slightly different bond lengths and bond angles due, in part, to the differing numbers and types of molecules of solvation, not *exactly* mirror images.

Solution and solid-state CD spectra for both complexes are given in Figure 3 and clearly show the mirror-imaging expected for what are, essentially, enantiomers. In both states the **Λ-*R,R*-III** isomer shows a (+, −, +) pattern of Cotton effects with the **Δ-*S,S*-III** isomer showing the opposite (−, +, −) pattern (λ and $\Delta\varepsilon$ values are given in the Experimental Section). In solution, peaks are seen at 320, 370, and 435 nm, and on the whole the solution and solid-state spectra are similar; however, the solid-state spectra show an extra peak/shoulder at 338 nm with the peak at 370 nm (in solution) shifted to 377 nm (solid-state). While shifts in Cotton-effect peaks between solution and solid-state measurements are not unusual and can be significant,[17] the extra peak/shoulder at 338 nm in the solid-state spectrum is presumably due to the two different molecules of the structure seen in the unit cell. In solution, the bond length and angle differences (partly due to the differing molecules of solvation) would seem to average out, and only one peak (370 nm) in this region, is seen.

*3.2.3. [Λ-Ru(η^2-$O_2CC_6H_5$)(η^2-S,S-o-tolyl-Dipamp)$_2$](PF$_6$), "**Λ-*S,S*-IV**" and [Δ-Ru(η^2-$O_2CC_6H_5$)(η^2-R,R-o-tolyl-Dipamp)$_2$]-(PF$_6$), "**Δ-*R,R*-IV**".* Figure 4 shows the molecular structures (and selected bond lengths and angles) of "**Λ-*S,S*-IV**" and "**Δ-*R,R*-IV**" and confirms the absolute configurations with Flack parameter values of 0.07(2) and −0.009(16) respectively. Both complexes crystallize in the chiral orthorhombic $C222_1$

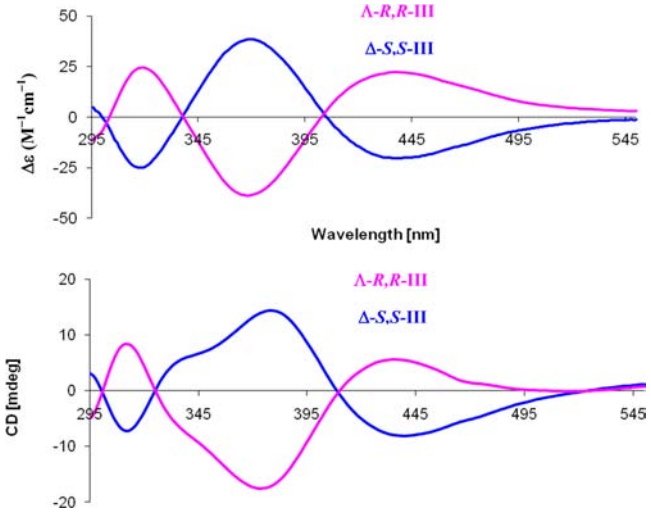

Figure 3. Solution (top) and solid-state (bottom) circular dichroism spectra of complexes **Λ-*R,R*-III** and **Δ-*S,S*-III**.

dx.doi.org/10.1021/ic401908t | *Inorg. Chem.* 2013, 52, 11563−11572

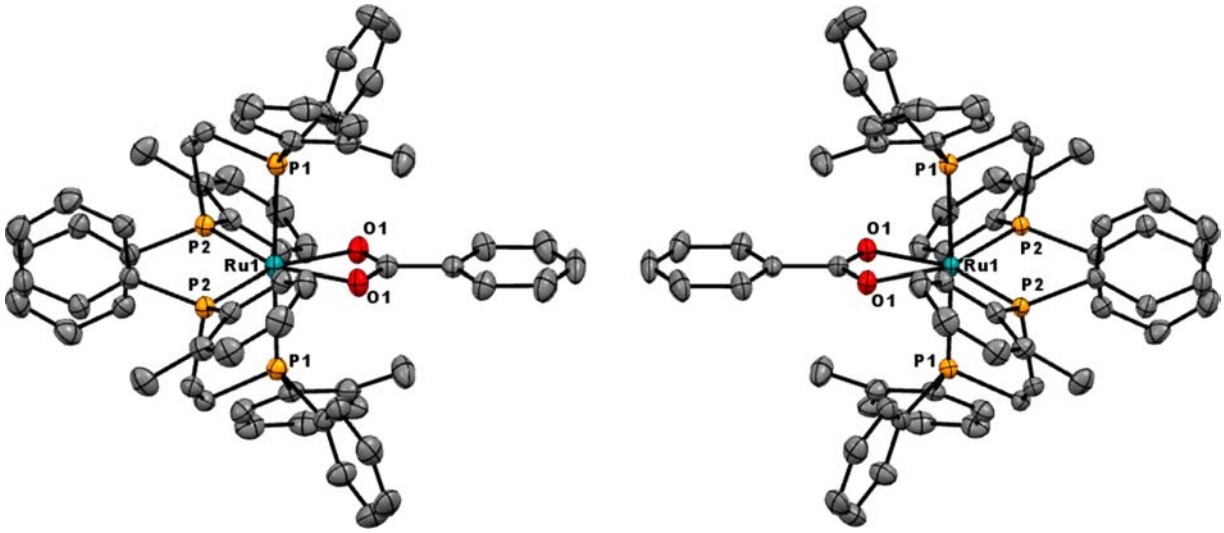

Figure 4. Molecular structure of "[**Λ-*S,S*-IV**]$^{+}$" (left) and "[**Δ-*R,R*-IV**]$^{+}$" (right). Hydrogen atoms and PF_6^- ions are omitted for clarity. Selected bond lengths (Å) and angles (°) for "[**Λ-*S,S*-IV**]$^{+}$": Ru(1)−O(1) 2.1824(17), Ru(1)−P(1) 2.4299(6), Ru(1)−P(2) 2.3387(7); O(1)−Ru(1)−O(1) 59.99(9), P(1)−Ru(1)−P(2) 81.54(2), O(1)−Ru(1)−P(1) 89.10(5), O(1)−Ru(1)−P(2) 160.44(5). For "[**Δ-*R,R*-IV**]$^{+}$": Ru(1)−O(1) 2.1840(12), Ru(1)−P(1) 2.4213(4), Ru(1)−P(2) 2.3401(5); O(1)−Ru(1)−O(1) 59.78(7), P(1)−Ru(1)−P(2) 81.598(15), O(1)−Ru(1)−P(1) 88.99(3), O(1)−Ru(1)−P(2) 160.34(3).

space group, and the bond lengths and angles are essentially identical (within error) so that we can safely classify these as enantiomers in the solid state. However, a major difference in these cases is that the *S,S* and *R,R* forms of the ligand have induced a different chirality at the metal from those seen for complex **III**; i.e., *S,S-o-tolyl*-Dipamp induces Λ chirality at the metal (instead of Δ), and *R,R-o-tolyl*-Dipamp induces Δ chirality (instead of Λ). So an "inversion" of chirality occurs at the metal when the stereogenic center on the ligand binds *directly* to the metal as opposed to being located on the spacer group *between* the two binding atoms. It is not clear why this occurs, and it could simply be due to the difference in the position of the stereocenter on the ligand. To add to the confusion, when one formally names the new complexes the *S* and *R* designations should actually become reversed (according to the Cahn−Ingold−Prelog naming system)[18] from the free ligands since the lone electron pair on the chiral phosphorus center is now bound to the metal center, making it the highest "priority" direction instead of the lowest. This is why we have designated the names of complexes **IV** and **V** (vide infra) with quotations. (This is an after the event effect and does not change the fact that we have inversion of the chiral induction in these cases with respect to the Chiraphos disassemblies.) Additional reactions with chirality at the metal-binding atom will need to be explored to see how general this "inversion" is.

The solution and solid-state CD spectra (Figure 5) show the typical mirror-imaging of Cotton-effects, thus confirming the absolute configurations and their predominance in both media again. Here "**Λ-*S,S*-IV**" shows a (+, −, +) pattern, and "**Δ-*R,R*-IV**" displays the opposite (−, +, −) trend. The spectra for the Λ and Δ forms show a similar pattern to what we saw for the Λ and Δ forms of complex **III** (Figure 4) except, of course, they are generated by ligands with the opposite (initial) chirality at a different pair of stereogenic centers (*o-tolyl*-Dipamp versus Chiraphos). A fourth relatively weak ($\Delta\varepsilon$ = 2−3 M^{-1} cm^{-1}) Cotton effect is seen only in the solution CD spectra at 448 nm. Its origin is unknown but could be due to a weak d−d transition buried under the mlct band. The inversion of chiral

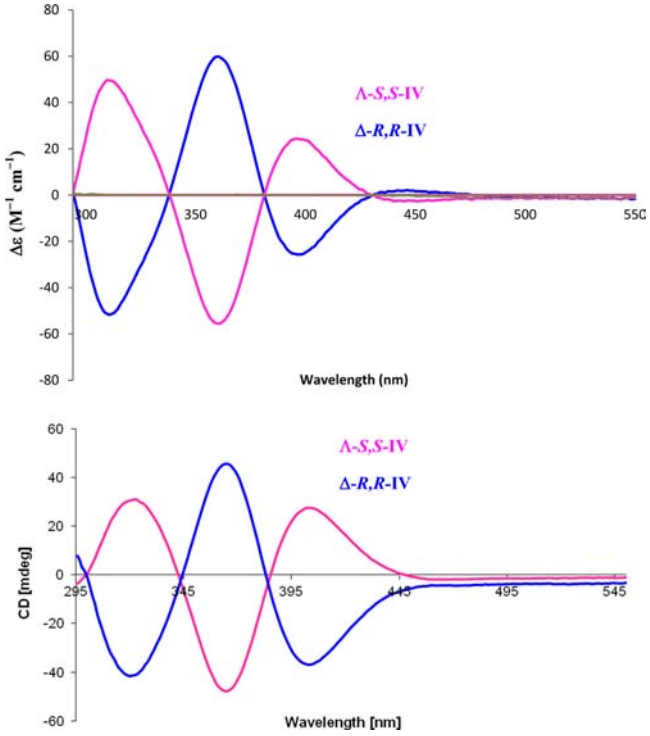

Figure 5. Solution (top) and solid-state (bottom) circular dichroism spectra of complexes "**Λ-*S,S*-IV**" and "**Δ-*R,R*-IV**".

induction that we saw in the X-ray structure is confirmed here as well, as the *S,S* ligand induces Λ chirality at the Ru(II) (not Δ like the *S,S*-Chiraphos in complex **III**), and the signal in the CD is similar to that of the *R,R*-Chiraphos complex in **III** (which induces Λ chirality at the Ru(II)).

*3.2.4. [Λ-Ru(η^2-O_2CCH_3)(η^2-S,S-o-tolyl-Dipamp)$_2$](PF$_6$), "**Λ-S,S-V**" and [Δ-Ru(η^2-O_2CCH_3)(η^2-R,R-o-tolyl-Dipamp)$_2$](PF$_6$), "**Δ-R,R-V**".* We were also able to synthesize the acetate derivatives of complex **IV** in a similar fashion (using [Ru_2(μ-O_2CCH_3)$_4$(MeOH)$_2$](PF$_6$) instead of [Ru_2(μ-$O_2CC_6H_5$)$_4$-

dx.doi.org/10.1021/ic401908t | *Inorg. Chem.* 2013, 52, 11563−11572

$(MeOH)_2](PF_6)$ and reacting it with the *S,S* and *R,R-o-tolyl*-Dipamp as before); however, we were unable to obtain single crystals of suitable quality for X-ray analysis despite our confidence in the compounds' purity from the elemental analysis, IR and electronic spectra, ^{31}P NMR and the CD spectra. The solution CD spectra of the two complexes can be seen in Figure S3 and looks remarkably similar to those seen for "**Λ-*S,S*-IV**" and "**Δ-*R,R*-IV**". The solid-state spectra are identical to the solution spectra shown. We conclude from this that our assignments are correct and that chiral induction occurs in a similar diastereoselective fashion for complexes **V** as for complexes **IV**.

3.2.5. Λ-(Acetato-O,O′)-bis(R-1,2-bis(diphenylphosphino)-propane-P,P′)ruthenium(II) Hexafluorophosphate, [Λ-Ru(η^2-O_2CCH_3)(R-Prophos)$_2$](PF$_6$), **Λ-*R*-VI.** Finally, with only one chiral center, the *R*-Prophos ligand induced Λ chirality at the Ru(II), similar to the *R,R*-Chiraphos ligand, to give **Λ-*R*-VI**. The structure of **Λ-*R*-VI** is shown in Figure 6, and it crystallizes

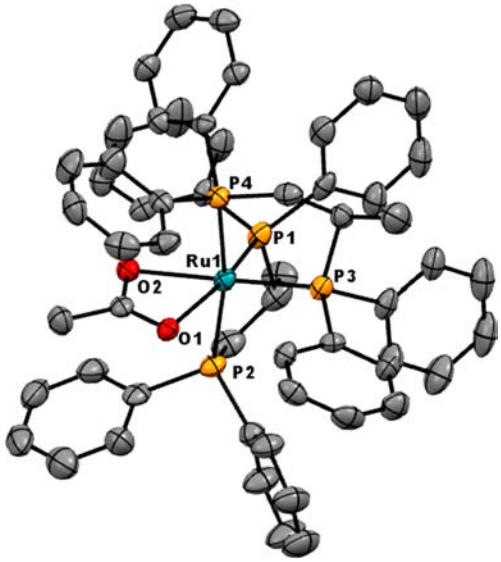

Figure 6. Molecular structure of **Λ-*R*-VI**$^+$. Hydrogen atoms and PF_6^- ions are omitted for clarity. Selected bond lengths (Å) and angles (°): Ru(1)−O(1) 2.189(3), Ru(1)−O(2) 2.178(3), Ru(1)−P(1) 2.3103(13), Ru(1)−P(2) 2.3839(13), Ru(1)−P(3) 2.3087(13), Ru(1)−P(4) 2.3670(13); O(1)−Ru(1)−O(2) 59.48, P(1)−Ru(1)−P(2) 83.58(5), P(3)−Ru(1)−P(4) 84.10(5), O(1)−Ru(1)−P(3) 106.45(9), O(2)−Ru(1)−P(4) 83.55(9), P(1)−Ru(1)−P(3) 90.51(5), P(2)−Ru(1)−P(4) 169.80(4).

in the chiral monoclinic space group $P2_1$ with a Flack parameter of −0.04(3). It is clear from the structure that the preferred geometrical isomer has the methyl groups adjacent to the phosphorus atoms that lie trans to the carboxylate oxygens. Multiple structural determinations on different synthetic batches all gave the same geometrical diastereomer. Attempts to isolate some of the other minor isomers from the crude reaction mixture, as seen in the ^{31}P NMR before recrystallization (Figure S4), failed to produce significant material for X-ray structural analysis. Work is ongoing in this area.

The solution CD spectra of **Λ-*R*-VI** mimics that of **Λ-*R,R*-III** as expected with a (+,−,+) pattern of Cotton effects at 311, 352, and 392 nm, respectively. The solid state CD is quite similar (Cotton effects at 308, 349, and 386 nm) and again verifies the similarity of the predominant chiral species in the solid and solution phases. The CD spectra are shown in Figure 7.

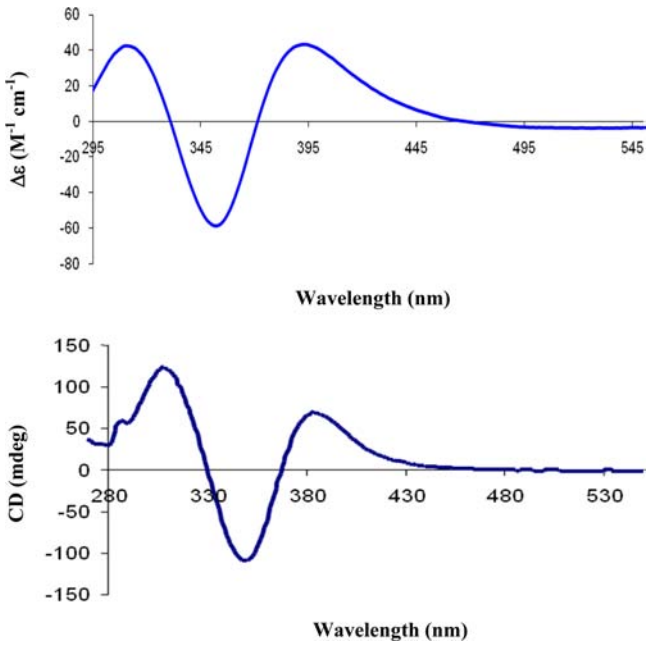

Figure 7. Solution (top) and solid-state (bottom) circular dichroism spectra for complex **Λ-*R*-VI**$^+$.

4. CONCLUSION

Table 2 summarizes and compares our results for complexes from the current paper and the previous communication.[7] It

Table 2. Yields and Absolute Configurations of Complexes

[Ru(η^2-P-P)(η^2-O_2CR)](PF$_6$) P−P, R	yield (%)	absolute configuration[a]	ref
Dppe, -C_6H_5 (**II**)	93	Λ, Δ	this work
R,R-Chiraphos, -CH_3	82	Λ	7
S,S-Chiraphos, -CH_3	84	Δ	7
R,R-Chiraphos, -C_6H_5 (**Λ-*R,R*-III**)	86	Λ	this work
S,S-Chiraphos, -C_6H_5 (**Δ-*S,S*-III**)	95	Δ	this work
R,R-o-tolyl-Dipamp, -CH_3 (**Δ-*R,R*-V**)	84	Δ[b]	this work
S,S-o-tolyl-Dipamp, -CH_3 (**Λ-*S,S*-V**)	89	Λ[b]	this work
R,R-o-tolyl-Dipamp, -C_6H_5 (**Δ-*R,R*-IV**)	87	Δ	this work
S,S-o-tolyl-Dipamp, -C_6H_5 (**Λ-*S,S*-IV**)	85	Λ	this work
R-Prophos, -CH_3 (**Λ-*R*-VI**)	79	Λ	this work

[a]Absolute configuration at the Ru(II) center. [b]Implied from other data as no X-ray structure was possible.

should be noted that in all cases but one the yields are >80%. The exception, **Λ-*R*-VI**, being slightly lower presumably due to the number of minor geometrical isomers that form in the original preparation but are not recoverable upon crystallization.

In this paper, we have extended our methodological work from an earlier communication to include a change in the

dx.doi.org/10.1021/ic401908t | *Inorg. Chem.* 2013, 52, 11563−11572

carboxylate R group, a change in the position of the chiral centers on the disassembling diphosphine, as well as a change in the number of chiral centers on the diphosphine. In each of these cases, we get very high diastereoselectivity, with disassemblies involving *S,S* and *R,R*-Chiraphos and *R*-Prophos leading to the induction of Δ, Λ, and Λ octahedral chirality at the Ru(II) center, respectively, whereas the *S,S* and *R,R-o-tolyl*-Dipamp ligands (chiral centers are the *coordinating* phosphorus atoms) leading to the opposite chirality, namely, Λ and Δ, respectively (see Table 2). The predominant species in solution correlate well with the isolated solids for which X-ray structures, in most cases, have been determined. We believe this methodology of chiral induction to be a very powerful, facile, and efficient route to novel, chiral-at-metal species.

We are currently investigating the asymmetric catalytic potential of these complexes and attempting further, similar, chiral induction reactions involving chiral N−N and P−N donor ligands, the latter of which can be made hemilabile to increase their potential catalytic effect.

■ ASSOCIATED CONTENT

Ⓢ Supporting Information

^{31}P NMR of complex **Δ-*S,S*-III** (**Λ-*R,R*-III**) and crude **Λ-*R*-VI**, UV−vis spectrum of "**Δ-*R,R*- IV**" ("**Λ-*S,S*-IV**"), CD spectra of "**Δ-*R,R*-V**" and "**Λ-*S,S*-V**", and X-ray crystallographic details (CIF) for **II·MeOH**, **Δ-*S,S*-III·1.875 MeOH**, **Λ-*R,R*-III·2.75 EtOH**, "**Λ-*S,S*-IV**", "**Δ-*R,R*-IV**", and **Λ-*R*-VI**. This material is available free of charge via the Internet at http://pubs.acs.org.

■ AUTHOR INFORMATION

Corresponding Author

*E-mail: maquino@stfx.ca.

Notes

The authors declare no competing financial interest.

■ ACKNOWLEDGMENTS

This work was supported by a Discovery Grant (M.A.S.A.) from the Natural Sciences and Engineering Council of Canada, NSERC (Canada). M.A.S.A. would also like to thank Dr. Brian MacLean for assistance with the circular dichroism spectra.

■ REFERENCES

(1) For example: (a) Constable, E. *Chem. Soc. Rev.* **2013**, *42*, 1637. (b) Pérez-García, L.; Amabilino, D. B. *Chem. Soc. Rev.* **2007**, *36*, 941. (c) Wenzel, T. J.; Wilcox, J. D. *Chirality* **2003**, *15*, 256. (d) Lennartson, A. *Inorg. Chim. Acta* **2011**, *365*, 451. (e) Yoshinari, N.; Konno, T. *Inorg. Chem.* **2008**, *47*, 7450. (f) Yamamoto, S.; Bouř, P. *Angew. Chem., Int. Ed.* **2012**, *51*, 11058. (g) Gugger, P.; Limmer, S. O.; Watson, A. A.; Willis, A. C.; Wild, S. B. *Inorg. Chem.* **1993**, *32*, 5692. (h) Bookham, J. L.; MacFarlane, W. *J. Chem. Soc., Chem. Commun.* **1993**, 1352. (i) Hua, X.; von Zelewsky, A. *Inorg. Chem.* **1991**, *30*, 3796.

(2) Smirnoff, A. P. *Helv. Chim. Acta* **1920**, *3*, 177.

(3) (a) Knof, U.; von Zelewsky, A. *Angew. Chem., Int. Ed.* **1999**, *38*, 303. (b) von Zelewsky, A. *Coord. Chem. Rev.* **1999**, *190−192*, 811. (c) von Zelewsky, A.; Mamula, O. *J. Chem. Soc., Dalton Trans.* **2000**, 219. (d) Quinodoz, B.; Labat, G.; Stoeckli-Evans, H.; von Zelewsky, A. *Inorg. Chem.* **2004**, *43*, 7994. (e) Mamula, O.; von Zelewsky, A.; Bark, T.; Bernardinelli, G. *Angew. Chem., Int. Ed.* **1999**, *38*, 2945. (f) Lötscher, D.; Rupprecht, S.; Collomb, P.; Belser, P.; Viebrock, H.; von Zelewsky, A.; Burger, P. *Inorg. Chem.* **2001**, *40*, 5675. (g) Perret-Aebi, L. E.; von Zelewsky, A.; Neels, A. *New J. Chem.* **2009**, *33*, 462. (h) Mürner, H.; Belser, P.; von Zelewsky, A. *J. Am. Chem. Soc.* **1996**, *118*, 7989. (i) Mürner, H.; von Zelewsky, A.; Stoeckli-Evans, H. *Inorg. Chem.* **1996**, *33*, 3931. (j) Hayes, P.; von Zelewsky, A.; Stoeckli-Evans, H. *J. Am. Chem. Soc.* **1993**, *115*, 5111.

(4) (a) Gong, L.; Mulcahy, S. P.; Harms, K.; Meggers, E. *J. Am. Chem. Soc.* **2009**, *131*, 9602. (b) Meggers, E. *Chem.—Eur. J.* **2010**, *16*, 752. (c) Meggars, E. *Eur. J. Inorg. Chem.* **2011**, 2911. (d) Gong, L.; Lin, Z.; Harms, K.; Meggers, E. *Angew. Chem., Int. Ed.* **2010**, *49*, 7955. (e) Gong, L.; Mulcahy, S. P.; Devarajan, D.; Harms, K.; Frenking, G.; Meggers, E. *Inorg. Chem.* **2010**, *49*, 7692. (f) Lin, Z.; Celik, M. A.; Harms, K.; Frenking, G.; Meggers, E. *Chem.—Eur. J.* **2011**, *17*, 12602. (g) Gong, L.; Müller, C.; Celik, M. A.; Frenking, G.; Meggers, E. *New J. Chem.* **2011**, 788. (h) Wenzel, M.; Meggers, E. *Eur. J. Inorg. Chem.* **2012**, 3168. (i) Chen, L. A.; Ma, J.; Celik, M. A.; Yu, H. L.; Cao, Z.; Frenking, G.; Gong, L.; Meggers, E. *Chem. Asian J.* **2012**, 2523. (j) Fu, C.; Wenzel, M.; Treutlein, E.; Harms, K.; Meggers, E. *Inorg. Chem.* **2012**, *51*, 10004.

(5) (a) Fontecave, M.; Hamelin, O.; Ménage, S. *Top. Organomet. Chem.* **2005**, *15*, 271. (b) Crassous, J. *Chem. Soc. Rev.* **2009**, *38*, 830. (c) Crassous, J. *Chem. Commun.* **2012**, *48*, 9684. (d) Train, C.; Gruselle, M.; Verdaguer, M. *Chem. Soc. Rev.* **2011**, *40*, 3297. (e) Pieraccini, S.; Masiero, S.; Ferrarini, A.; Spada, G. P. *Chem. Soc. Rev.* **2011**, *40*, 258. (f) Morris, R. E.; Bu, X. *Nature Chem.* **2010**, *2*, 353. (g) Xu, J.; Wang, R.; Li, Y.; Gao, Z.; Yao, R.; Wang, S.; Wu, B. *Eur. J. Inorg. Chem.* **2012**, 3349. (h) Miyake, H.; Tsukube, H. *Chem. Soc. Rev.* **2012**, *41*, 6977. (i) Brahma, S.; Ikbal, Sk.A.; Dey, S.; Rath, S. P. *Chem. Commun.* **2012**, *48*, 4070. (j) Zhou, P.; Li, H. *Dalton Trans.* **2011**, *40*, 4834. (k) Haberhauer, G. *Angew. Chem., Int. Ed.* **2010**, *49*, 9286. (l) Canary, J. W.; Mortezaei, S.; Liang, J. *Coord. Chem. Rev.* **2010**, *254*, 2249.

(6) (a) Wyman, I. W.; Burchell, T. J.; Robertson, K. N.; Cameron, T. S.; Swarts, J. C.; Aquino, M. A. S. *Organometallics* **2004**, *23*, 5353. (b) Wyman, I. W.; Robertson, K. N.; Cameron, T. S.; Swarts, J. C.; Aquino, M. A. S. *Organometallics* **2005**, *24*, 6055. (c) Wyman, I. W.; Robertson, K. N.; Cameron, T. S.; Swarts, J. C.; Aquino, M. A. S. *Inorg. Chim. Acta* **2006**, *359*, 3092. (d) Murray, A. H.; Yue, Z.; Wallbank, A. I.; Cameron, T. S.; Vadavi, R.; MacLean, B. J.; Aquino, M. A. S. *Polyhedron* **2008**, *27*, 1270.

(7) Vadavi, R.; Conrad, E. D.; Arbuckle, D. I.; Cameron, T. S.; Essoun, E.; Aquino, M. A. S. *Inorg. Chem.* **2011**, *50*, 11862.

(8) (a) Drysdale, K. D.; Beck, E. J.; Cameron, T. S.; Robertson, K. N.; Aquino, M. A. S. *Inorg. Chim. Acta* **1997**, *256*, 243. (b) Chakravarty, A. R.; Das, B. K. *Polyhedron* **1988**, *9*, 685.

(9) Cooke, M. W.; Cameron, T. S.; Robertson, K. N.; Swarts, J. C.; Aquino, M. A. S. *Organometallics* **2002**, *21*, 5962.

(10) *Bruker AXS Crystal Structure Analysis Package: Bruker (2000), SHELXTL. Version 6.14. Bruker (2005). XPREP. Version 2005/2. Bruker (2005). SAINT. Version 7.23 A. Bruker (2006). APEX2. Version 2.0-2.* Bruker AXS Inc., Madison, Wisconsin, USA.

(11) Cromer, D. T.; Waber, J. T. *International Tables for X-ray Crystallography*; Kynoch Press: Birmingham, UK, 1974; Vol. *4*, Table 2.2 A.

(12) van der Sluis, P.; Spek, A. L. *Acta Crystallogr.* **1990**, *A46*, 194.

(13) Nakamoto, K. *Infrared and Raman Spectra of Inorganic and Coordination Compounds*; Wiley Interscience, New York, 1997.

(14) Diphosphines, such as 1,1-bis(diphenylphosphino) methane (dppm), that form four-membered metallacycles with Ru(II) show their doublet of triplets in the range: −13.7 to −18.0 ppm (triplet, 2P's *trans* to P) and −5.7 to +3.7 ppm (triplet, 2P's *trans* to O). Six-membered ring systems formed by 1,3-bis(diphenylphosphino) propane, for example, show a doublet of triplets in the range: 2.6 to 4.1 ppm (triplet, 2P's *trans* to P) and 22.4 to 31.2 ppm (triplet, 2P's *trans*to O). Both of these ranges are quite distinct from that seen in the five-membered ring systems discussed in this paper. See ref 6a for further detail.

(15) Yamaguchi, M.; Yabuki, M.; Yamagishi, T.; Kondo, M.; Kitagawa, S. *J. Organomet. Chem.* **1997**, *538*, 199.

(16) (a) Flack, H. D.; Bernardenelli, G. *J. Appl. Crystallogr.* **2000**, *33*, 1143. (b) Flack, H. D.; Bernardenelli, G. *Acta Crystallogr. Sect. A.* **1999**, No. 55, 908.

(17) Castiglioni, E.; Abbate, S.; Longhi, G.; Gangemi, R. *Chirality* **2007**, *19*, 491.
(18) (a) Cahn, R. S.; Ingold, C. K.; Prelog, V. *Angew. Chem., Int. Ed.* **1966**, *5*, 385. (b) Prelog, V.; Helmchen, G. *Angew. Chem., Int. Ed.* **1982**, *21*, 567.